

## ELECTRON MICROSCOPIC AND INFRARED SPECTRAL STUDIES ON THE STRUCTURE OF ALUMINA PHASES

Seiji KIMURA<sup>1</sup>, Kazuhiko KAMEI<sup>1</sup>, Noritoshi TSUDA<sup>1</sup>, Yoshio SAITO<sup>2</sup>,  
Chiyoë KOIKE<sup>3</sup> and Chihiro KAITO<sup>1</sup>

<sup>1</sup>*Department of Physics, Ritsumeikan University, Kusatsu, Shiga 525*

<sup>2</sup>*Department of Electronics and Information Science, Kyoto Institute of Technology,  
Matsugasaki, Sakyo-ku, Kyoto 606*

<sup>3</sup>*Department of Physics, Kyoto Pharmaceutical University, Yamashina, Kyoto 607*

**Abstract:** Alumina produced by oxidation of aluminum in air was studied by infrared spectroscopy and electron microscopy. Infrared spectra of both alumina particles and alumina film oxidized in air showed an absorption peak at 10.8  $\mu\text{m}$ , though that of  $\gamma\text{-Al}_2\text{O}_3$  particles showed a broad 13  $\mu\text{m}$  peak. On the basis of the infrared spectra and electron diffraction pattern, it was concluded that alumina produced by the oxidation of aluminum in air is  $\eta\text{-Al}_2\text{O}_3$ . The phase transition from  $\eta$ -phase to  $\gamma$ -phase and to  $\alpha$ -phase took place at 900°C and 1100°C, respectively. The relationships between infrared spectra and crystal structure of some alumina phases are discussed.

### 1. Introduction

Corundum ( $\text{Al}_2\text{O}_3$ ) is the refractory phase predicted to condense first from a cooling gas of solar composition before the appearance of minerals such as perovskite, melilite and spinel (GROSSMAN, 1972). According to the condensation theory, it is suggested that corundum disappears at 1240°C due to the formation of spinel. Actually, corundum had not been reported their existence in meteorites until quite recently. However, numerous twenty-six corundum grains were found in the Murchison C2 chondrites, ranging in size from 3 to 15  $\mu\text{m}$  (ANDERS *et al.*, 1991). The analysis of grains by ion microprobe mass spectrometry indicated the existence of <sup>26</sup>Al and <sup>16</sup>O in the early solar system. Moreover, the presence of corundum grains in space is also suggested from astronomical observation and theoretical calculations (VARDYA *et al.*, 1986; ONAKA *et al.*, 1989; KOZASA *et al.*, 1989). For example, the broad 12  $\mu\text{m}$  feature observed in a spectra of Mira variables is identified as a characteristic band of aluminum oxide grains. It is also suggested that corundum grains may have condensed in the ejecta of SN 1987A. However, it is not obvious at present whether alumina grains in the ejecta of SN 1987A are amorphous or crystalline, or whether they are  $\alpha\text{-Al}_2\text{O}_3$  or  $\gamma\text{-Al}_2\text{O}_3$ . In spite of increasing interest in optical constants of alumina grains, very few spectral studies of alumina grains have been performed thus far. In a previous study, spectra of two types of  $\gamma\text{-Al}_2\text{O}_3$  particles were measured (KOIKE *et al.*, 1995). The spectra showed very broad peaks around 13  $\mu\text{m}$ . It was shown that the features agreed very well with those of spectra calculated using bulk data of amorphous  $\gamma\text{-Al}_2\text{O}_3$ . In general, it is well known that  $\gamma\text{-Al}_2\text{O}_3$  can be produced by many techniques including vacuum evaporation of  $\text{Al}_2\text{O}_3$ , sputtering, chemi-

cal vapor deposition, anodization to form barrier-type coatings and oxidation of aluminum. However, in the present experiment, it is shown that alumina produced by the oxidation of metallic aluminum in air is not  $\gamma$ - $\text{Al}_2\text{O}_3$  but  $\eta$ - $\text{Al}_2\text{O}_3$ , and that the  $\eta$ - $\text{Al}_2\text{O}_3$  phase is transformed to  $\gamma$ - $\text{Al}_2\text{O}_3$  or  $\alpha$ - $\text{Al}_2\text{O}_3$  by heating above  $900^\circ\text{C}$ . Various alumina particles and alumina films have been studied by infrared (IR) spectroscopy. The relationships between IR spectrum and the crystal structure of alumina particles and alumina film are also discussed.

## 2. Experiments

At first Al particles and Al film were prepared by the gas evaporation method and vacuum evaporation method, respectively. Al particles were produced by evaporating metallic aluminum in Ar gas of pressure about 13 kPa. Al particles were oxidized by heating in air at  $400$ – $1100^\circ\text{C}$  for 20 hours. For electron microscopic analysis, particles were dispersed in ethyl alcohol and mounted on a standard electron microscopic grid covered with carbon film. Particles were also mixed into KBr powder in order to measure IR spectrum, then KBr pellets embedded the particles were formed using a tablet punching device. On the other hand, Al film was produced by evaporating metallic aluminum in vacuum of  $10^{-3}$  Pa on KBr substrate. The vacuum-evaporated Al film on KBr substrate was oxidized by heating in air at  $550^\circ\text{C}$  for several hours. In addition to those samples, two types of commercial alumina particles were examined. One is  $\gamma$ - $\text{Al}_2\text{O}_3$  particles from Nippon Aerosil Co. Ltd. The other is  $\alpha$ - $\text{Al}_2\text{O}_3$  sample from National Bureau of Standards, which is used as a standard sample for checking the intensity of X-ray diffraction pattern. The transmittance of KBr pellets was measured with a Fourier transform infrared spectrometer (Horiba Inc., FT-210). The observation of the specimens was carried out using Hitachi H-7100R and H-800 electron microscopes.

## 3. Results and Discussion

Figure 1 is electron microscopic (EM) images and electron diffraction (ED) patterns of Aerosil  $\gamma$ - $\text{Al}_2\text{O}_3$  particles and standard  $\alpha$ - $\text{Al}_2\text{O}_3$  sample. Aerosil  $\gamma$ - $\text{Al}_2\text{O}_3$  particles of a mean diameter 20 nm are spherical in shape. ED pattern in Fig. 1a shows strong rings due to  $\gamma$ - $\text{Al}_2\text{O}_3$  crystal and weak rings due to  $\alpha$ - $\text{Al}_2\text{O}_3$  crystal. This indicates that the particles are composed predominantly of  $\gamma$ - $\text{Al}_2\text{O}_3$  crystal and of a small amount of  $\alpha$ - $\text{Al}_2\text{O}_3$  crystal. As shown in Fig. 1b, the standard sample contains a small amount of  $\gamma$ - $\text{Al}_2\text{O}_3$  particles.  $\alpha$ - $\text{Al}_2\text{O}_3$  particles shown in Fig. 1b have size less than  $1\ \mu\text{m}$  and are spherical in shape. Small particles with a mean size of 30 nm pointed by arrows in Fig. 1b were identified as  $\gamma$ - $\text{Al}_2\text{O}_3$  structure by ED pattern of the region of the coagulated small particles. The IR spectrum of Aerosil  $\gamma$ - $\text{Al}_2\text{O}_3$  particles in Fig. 2 shows a very broad peak at about  $13\ \mu\text{m}$ . This feature agrees very well with that of the spectrum calculated using bulk data of amorphous  $\gamma$ - $\text{Al}_2\text{O}_3$  (KOIKE *et al.*, 1995). Characteristic absorption peaks appear at 13.7, 15.6, 17, 20.4 and  $22.4\ \mu\text{m}$  in the IR spectrum of the standard  $\alpha$ - $\text{Al}_2\text{O}_3$  sample.

Figure 3 shows IR spectra of Al film heated in air at  $550^\circ\text{C}$  for 5 hours (curve a) and Al particles heated in air at  $400^\circ\text{C}$  for 20 hours (curve b). The IR spectra of both film and

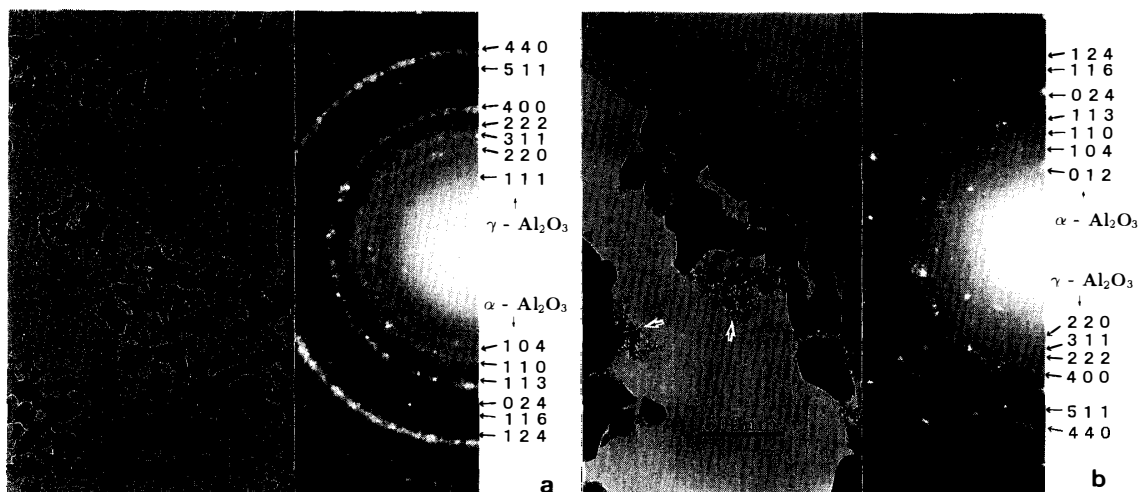


Fig. 1. EM images and ED patterns of (a) Aerosil  $\gamma$ - $\text{Al}_2\text{O}_3$  particles and (b) standard  $\alpha$ - $\text{Al}_2\text{O}_3$  sample.

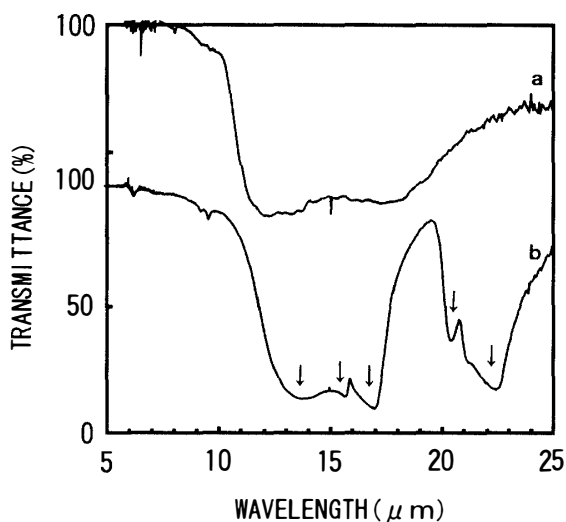


Fig. 2. IR spectra of (a) Aerosil  $\gamma$ - $\text{Al}_2\text{O}_3$  particles and (b) standard  $\alpha$ - $\text{Al}_2\text{O}_3$  sample. Typical peak positions of  $\alpha$ -phase are indicated in figure.

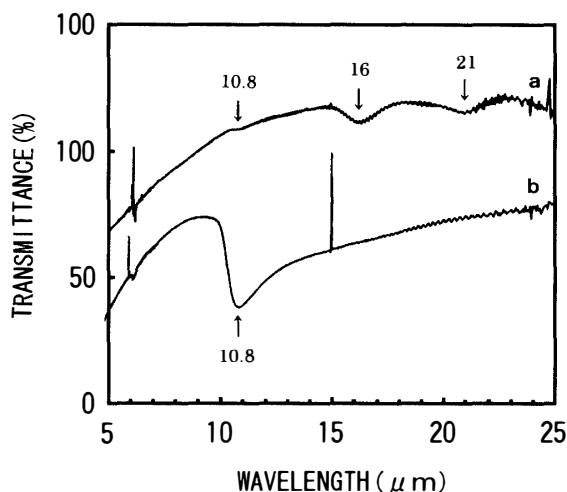


Fig. 3. IR spectra of (a) Al film heated in air at  $550^\circ\text{C}$  for 5 hours and (b) Al particles heated in air at  $400^\circ\text{C}$  for 20 hours. Peak positions are indicated by arrows.

particles have an absorption peak at  $10.8 \mu\text{m}$ , different from the IR spectrum of Aerosil  $\gamma$ - $\text{Al}_2\text{O}_3$  particles. In general, alumina produced by the oxidation of aluminum has been considered to be  $\gamma$ -alumina. The difference of the peak positions at  $13 \mu\text{m}$  (IR spectrum of Aerosil  $\gamma$ - $\text{Al}_2\text{O}_3$  particles) and  $10.8 \mu\text{m}$  (IR spectrum of alumina produced by the oxidation of aluminum) suggests that the structure of oxides produced from both metallic particles and film is neither  $\gamma$ - nor  $\alpha$ -structure.

Figure 4 is EM image and ED pattern of Al film heated in air at  $550^\circ\text{C}$  for 5 hours. ED pattern was indexed as the  $\eta$ -structure. Diffraction patterns of  $\eta$ -phase are very similar to that of  $\gamma$ -phase, because of the same cubic structure with nearly the same lattice constant. The difference of the structure may be due to the position of Al atoms, though

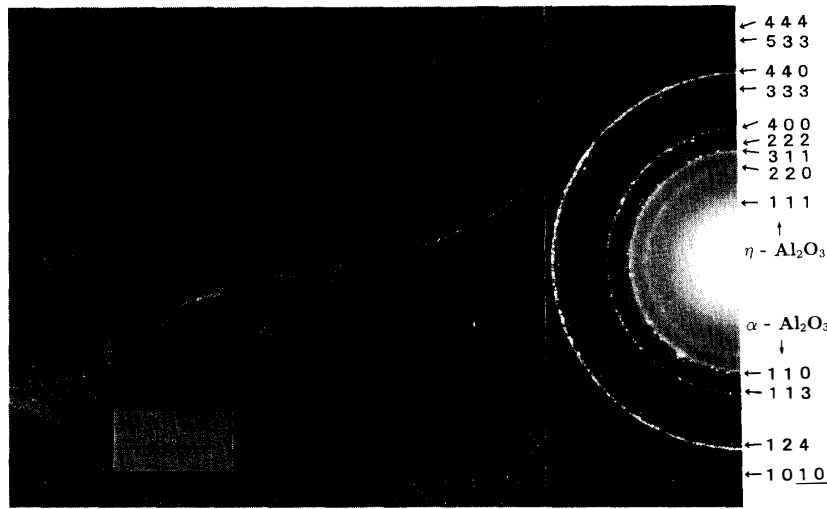


Fig. 4. EM image and ED pattern of Al film heated in air at 550°C for 5 hours. ED pattern can be indexed by η-phase.

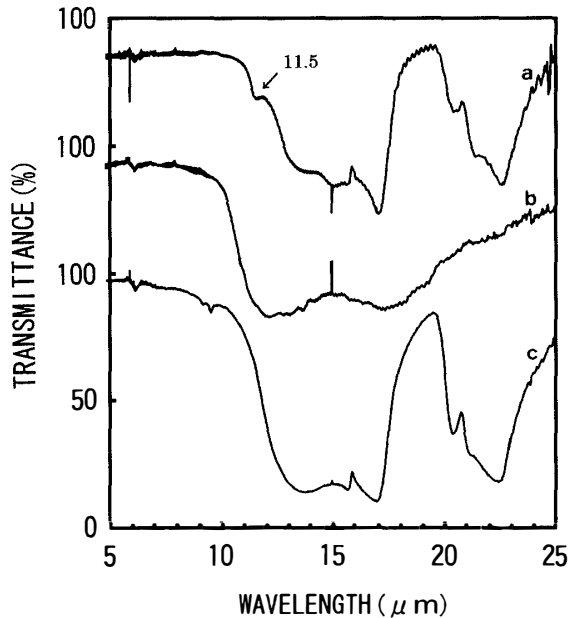


Fig. 5. IR spectra of (a) η-phase particles and (b) Aerosil γ-Al<sub>2</sub>O<sub>3</sub> particles heated at 1100°C for 20 hours. IR spectrum of (c) standard α-Al<sub>2</sub>O<sub>3</sub> sample is also shown.

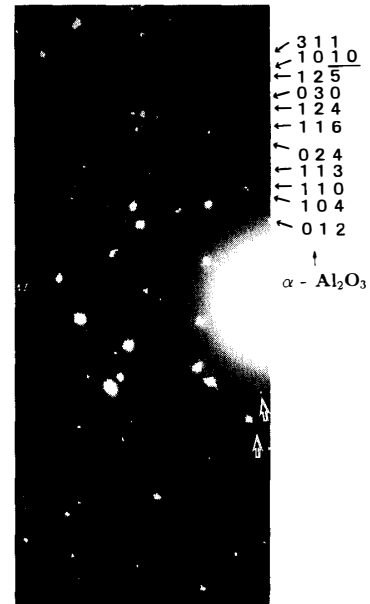


Fig. 6. ED pattern of η-phase particles heated in air at 1100°C for 20 hours. ED pattern shows the transformation to α-phase.

the fine structure of η-phase has not been clarified. On the basis of IR spectral data, it was concluded that alumina produced by the oxidation of aluminum in air is not γ-Al<sub>2</sub>O<sub>3</sub> but η-Al<sub>2</sub>O<sub>3</sub>. In addition to the absorption peak at 10.8 μm, the absorption peaks at 16 and 21 μm in curve a in Fig. 3 were observed. According to the theoretical calculation of PEARCE and EVANS (1984) for vacuum, the absorption peaks at 16 and 21 μm correspond to those of α-Al<sub>2</sub>O<sub>3</sub>. These peaks agreed well with two peaks measured using the standard α-Al<sub>2</sub>O<sub>3</sub> sample (Fig. 2). The appearance of the two peaks may be due to the preferred orientation of the oxide film on Al film. Appearance of α-Al<sub>2</sub>O<sub>3</sub> was also confirmed from ED pattern. Although the α-Al<sub>2</sub>O<sub>3</sub> has been considered to be a stable phase

above 1500°C, it turns out that a part of  $\eta$ -Al<sub>2</sub>O<sub>3</sub> film changes to  $\alpha$ -Al<sub>2</sub>O<sub>3</sub> upon heating at 550°C. Difference in the absorption peak between  $\alpha$ -Al<sub>2</sub>O<sub>3</sub> crystal from Al film and the standard  $\alpha$ -Al<sub>2</sub>O<sub>3</sub> sample is due to the measurement in vacuum (film) and in KBr medium.

The samples of  $\eta$ -phase particles and Aerosil  $\gamma$ -Al<sub>2</sub>O<sub>3</sub> particles were heated at 1100°C for 20 hours. IR spectra of those samples are shown in Fig. 5 together with that of the standard  $\alpha$ -Al<sub>2</sub>O<sub>3</sub> sample. The IR spectrum of the heated  $\eta$ -phase particles agrees very well with that of the standard  $\alpha$ -Al<sub>2</sub>O<sub>3</sub> sample, except for an absorption peak at 11.5  $\mu$ m. On the other hand, IR spectrum of Aerosil  $\gamma$ -Al<sub>2</sub>O<sub>3</sub> particles changed little. Figure 5 suggests that the structure of both particles heated in air is quite different from each other despite the same heat treatment. This result also supports the conclusion that alumina produced by the oxidation of aluminum is not  $\gamma$ -phase. From this experiment, it has been found that the phase transition from  $\eta$ -phase to  $\alpha$ -phase take place upon heating at 1100°C. ED pattern after heat treatment of  $\eta$ -phase is given in Fig. 6. In addition to the  $\alpha$ -phase, there exist two unidentified rings indicated by arrows except for  $\alpha$ -phase rings. Since alumina phases have many polytypes, a small amount of another phase may

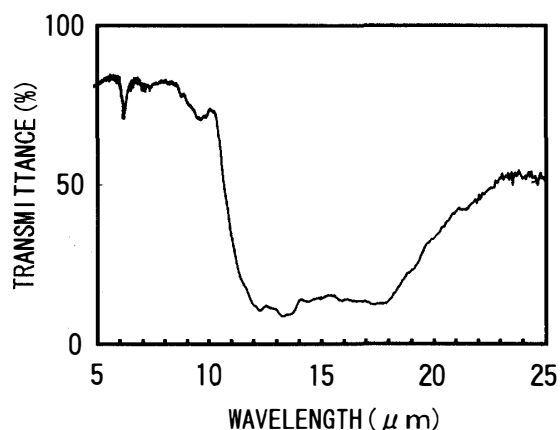


Fig. 7. IR spectrum of  $\eta$ -phase particles heated in air at 900°C for 20 hours. The spectrum indicates the phase transition to  $\gamma$ -phase.

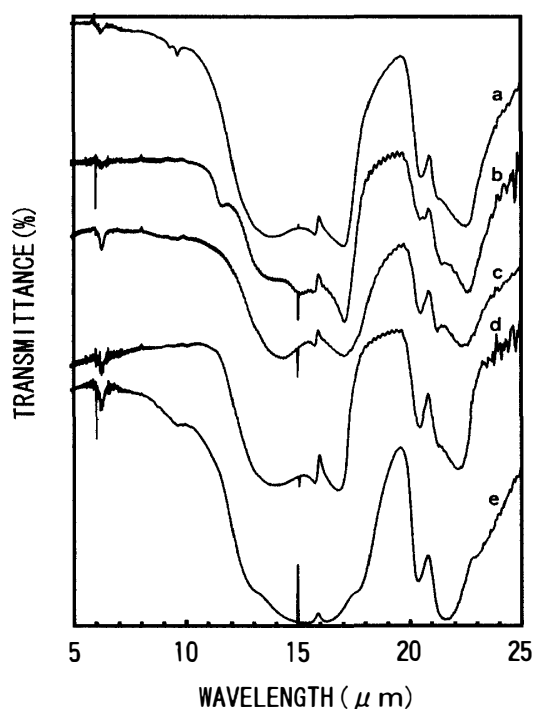


Fig. 8. IR spectra of  $\alpha$ -Al<sub>2</sub>O<sub>3</sub> particles produced under various experimental conditions. (a) the standard  $\alpha$ -Al<sub>2</sub>O<sub>3</sub> sample, (b)  $\eta$ -Al<sub>2</sub>O<sub>3</sub> particles heated in air at 1100°C for 20 hours, (c)  $\eta$ -Al<sub>2</sub>O<sub>3</sub> particles heated in Ar atmosphere at 1500°C for 10 hours, (d) Aerosil  $\gamma$ -Al<sub>2</sub>O<sub>3</sub> particles heated in Ar atmosphere at 1500°C for 1 min and (e) Aerosil  $\gamma$ -Al<sub>2</sub>O<sub>3</sub> particles heated in Ar atmosphere at 1500°C for 2 hours.

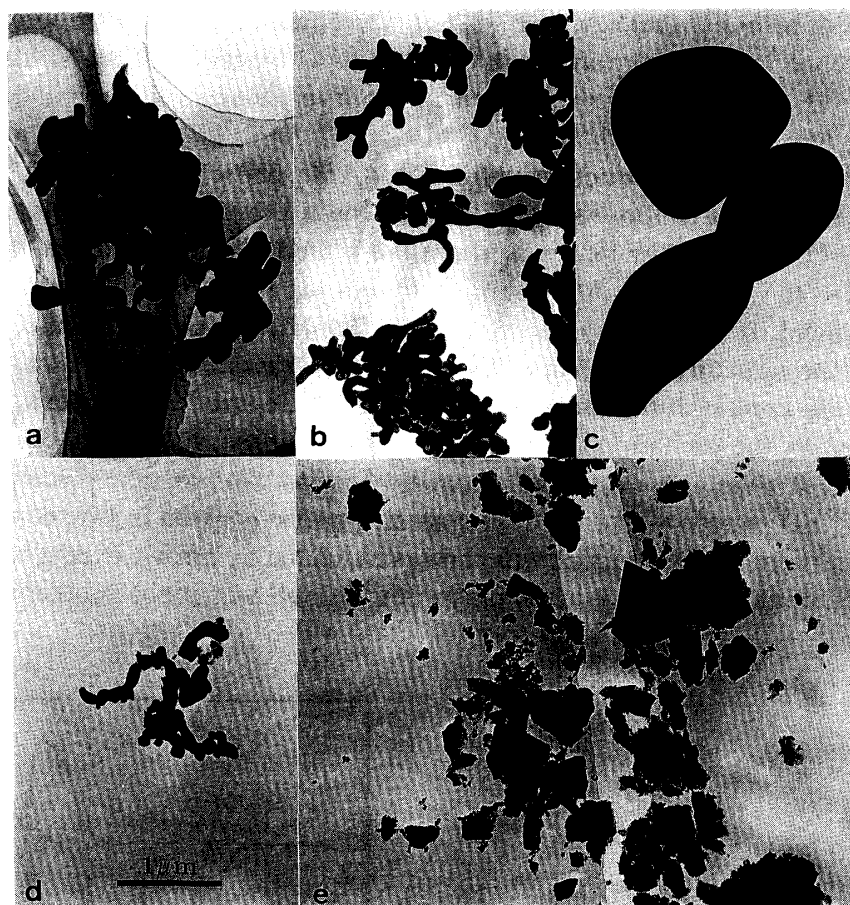


Fig. 9. EM images of  $\alpha\text{-Al}_2\text{O}_3$  particles produced under various experimental conditions. (a), (b), (c), (d) and (e) correspond to those indicated in Fig. 8. EM images are shown in the same scale.

appear upon heat treatment. Detailed analysis concerning this point is under way. The IR spectrum of  $\eta$ -phase particles heated at  $900^\circ\text{C}$  for 20 hours in air is shown in Fig. 7. It is in good agreement with that of Aerosil  $\gamma\text{-Al}_2\text{O}_3$  particles. Therefore, it can be concluded that the phase transition from  $\eta$ -phase to  $\gamma$ -phase takes place upon heating at  $900^\circ\text{C}$ .

In this experiment, IR spectra of many kinds of  $\alpha\text{-Al}_2\text{O}_3$  particles produced under a different growth condition were measured. Figures 8 and 9 show, respectively, IR spectra and EM images of the  $\alpha\text{-Al}_2\text{O}_3$  particles. Although ED patterns of these samples showed  $\alpha\text{-Al}_2\text{O}_3$  phase, the features of IR spectra differ as seen in Fig. 8. IR spectra for the same crystal habits and sizes agreed well as seen in Fig. 8a, b, d. When the size of the particles becomes larger, the  $17\ \mu\text{m}$  peak in the IR spectrum becomes broad as seen in Fig. 8. This result indicates that the difference of the particle size and the crystal shape can influence the spectral features. However, IR spectral studies on the size and shape effects of particles for a single material have been little studied. The details of these effects will be published elsewhere, including the variation of the absolute absorption values due to the shape effect.

The presence of alumina grains in various astronomical objects have been listed in

Table II in previous paper (KOIKE *et al.*, 1995). As suggested in that paper, besides Mira variables, new emission features have been observed at 7.15, 10, 11.5, 13.1, 18 and 19.7  $\mu\text{m}$  bands in other oxygen-rich circumstellar shells (GOEBEL *et al.*, 1994). The absorption peak of  $\eta$ ,  $\gamma$  and  $\alpha$  phases have been observed in the present experiments. Taking account of the shape effects in  $\alpha\text{-Al}_2\text{O}_3$  particle, except 7.15  $\mu\text{m}$  peak, all other peaks may be assigned as the alumina phases. The absolute values of these phases may become important to correlate between the observation data and laboratory data. Details will be published elsewhere, including the shape effect on the spectrum.

### Acknowledgments

This work was supported by a Grant-in-Aid for General Scientific Research (No.07409007, KAITO) and (No.07640539, KOIKE) from the Japanese Ministry of Education, Science and Culture.

### References

- ANDERS, E., VIRAG, A., ZINNER, E. and LEWIS, R.S. (1991):  $^{26}\text{Al}$  and  $^{16}\text{O}$  in the early solar system: Clues from meteoritic  $\text{Al}_2\text{O}_3$ . *Astrophys. J.*, **373**, L77–L80.
- GOEBEL, J. H., BREGMAN, J. D. and WITTEBORN, F. C. (1994): A 7 micron dust emission feature in oxygen-rich circumstellar shells. *Astrophys. J.*, **430**, 317–322.
- GROSSMAN, L. (1972): Condensation in the primitive solar nebula. *Geochim. Cosmochim. Acta*, **36**, 597–619.
- KOIKE, C., KAITO, C., YAMAMOTO, T., SHIBAI, H., KIMURA, S. and SUTO, H. (1995): Extinction spectra of corundum in the wavelengths from UV to FIR. *Icarus*, **114**, 203–214.
- KOZASA, T., HASEGAWA, H. and NOMOTO, K. (1989): Formation of dust grains in the ejecta of SN 1987A. *Astrophys. J.*, **344**, 325–331.
- ONAKA, T., DE JONG, T. and WILLEMS, F. J. (1989): A study of M Mira variables based on IRAS LRS observations. I. Dust formation in the circumstellar shell. *Astron. Astrophys.*, **218**, 169–179.
- PEARCE, G. and EVANS, A. (1984): The infra-red emission from a composite circumstellar dust shell heated by a supernova. *Astron. Astrophys.*, **136**, 306–312.
- VARDYA, M. S., DE JONG, T. and WILLEMS, F. J. (1986): IRAS Low-Resolution spectrograph observations of silicate and molecular SiO emission in Mira variables. *Astrophys. J.*, **304**, L29–L32.

(Received August 7, 1995; Revised manuscript accepted October 30, 1995)